ISSN 0016-7029, Geochemistry International, 2007, Vol. 45, No. 1, pp. 47–61. © Pleiades Publishing, Ltd., 2007.
Original Russian Text © A.S. Astakhov, K. Wallmann, M.V. Ivanov, G.M. Kolesov, V.V. Sattarova, 2007, published in Geokhimiya, 2007, No. 1, pp. 54–70.

# Distribution and Accumulation Rate of Hg in the Upper Quaternary Sediments of the Deryugin Basin, Sea of Okhotsk

**A. S. Astakhov[a], K. Wallmann[b], M. V. Ivanov[a], G. M. Kolesov[c], and V. V. Sattarova[a]**

[a] *V.I. Il'ichev Pacific Oceanological Institute, Far East Division, Russian Academy of Sciences, Baltiiskaya ul. 43, Vladivostok, 690041 Russia*
*e-mail: astakhov@poi.dvo.ru*
[b] *Leibniz Institute for Marine Sciences, Wischhofstrasse 1–3, Kiel, D-24148 Germany*
*e-mail: kwallmann@ifm-geomar.de*
[c] *Vernadsky Institute of Geochemistry and Analytical Chemistry, Russian Academy of Sciences, ul. Kosygina 19, Moscow, 11991 Russia*
*e-mail: drkolesov@mail.ru*

Received July 25, 2005

**Abstract**—The Hg distribution and some mineralogical–geochemical features of bottom sediments up to a depth of 10 m in the Deryugin Basin showed that the high and anomalous Hg contents in the Holocene deposits are confined to a spreading riftogenic structure and separate fluid vents within it. The accumulations of Hg in the the sediments were caused by its fluxes from gas and low-temperature hydrothermal vents under favorable oceanological conditions in the Holocene. The two mainly responsible for the high and anomalous Hg contents are infiltration (fluxes of hydrothermal or gas fluids from the sedimentary cover) and plume (Hg precipitation from water plumes with certain hydrochemical conditions forming above endogenous sources). The infiltration anomalies of Hg were revealed in the following environments: (1) near gas vents on the northeastern Sakhalin slope, where high Hg contents are associated only with Se and were caused by the accumulation of gases ascending from beneath the gas hydrate layer; (2) in the area of inferred occasionally operating low-temperature hydrothermal seeps in the central part of the Deryugin Basin, in which massive barite chimneys, hydrothermal Fe–Mn crusts, and anomalous contents of Mn, Ba, Zn, and Ni in sediments develop.

**DOI:** 10.1134/S0016702907010041

## INTRODUCTION

The study of Hg distribution in marine ecosystems is a very important problem, because Hg is an indicator of fluxes of endogenous fluids and an exploration sign of ore and hyhdrocabron deposits, as well as a dangerous and global environmental pollutant. The complicated character of this problem is determined by the high migration ability of Hg and its natural and anthropogenic sources. It is believed that most Hg (up to 90% [1]) in oceans and bottom sediments is supplied from the atmosphere, with some introduction from anthropogenic and other natural sources. The anthropogenic constituent in the atmospheric balance of Hg and its spatial and temporal variations have been studied in detail in [2]. However, the natural component was estimated only qualitatively, and no total Hg balance in the ocean (including its bottom fluxes) was evaluated.

The analysis of elevated Hg concentrations of natural origin in rocks showed that ore (related to the deposits of different composition) and non-ore (having only geochemical significance) concentrations are restricted to mantle-rooted mobile belts in continental and oceanic blocks of the Earth's crust [3]. A mantle origin is inferred for Hg at most ore deposits and gas fields, while Hg belts are confined to deep-seated fault zones. Natural geochemical cycles of Hg are controlled by the predominant removal of its vapor and diverse solutions from volcanoes along faults and fluid-conducting channels, defluidization of hydrocarbon and coal deposits, and removal from the supergene zone of sulfide deposits. This was long utilized in the mercurymetric prospectings of onshore ore deposits and oil–gas fields based on lithochemical, hydrochemical, and atmochemical dispersion halos [4].

Similar tendencies in Hg accumulation were found in active oceanic mantle-rooted structures. High Hg contents in sulfide ores and their host sediments were found in both midocean ridges [3, 5] and spreading zones in marginal basins [6]. The formation of anomalous and elevated Hg contents in bottom sediments at sea basins with insignificant anthropogenic pollution is determined mainly by its flux from the Earth's crust and precipitation near hydrothermal vents [4, 6]. Of great importance in this context is the character of hydrothermal vents, host rocks, and postsedimentation transformations. It was established that high Hg contents could be formed by fluid seeping through sedimentary sequence (infiltration) and during precipitation from aqueous plumes forming above an endogenous source (plumous) [5].

By analogy with onshore mercurymetric prospecting and available data on Hg distribution in marine sulfide ores and metalliferous sediments, elevated Hg concentrations in bottom sediments and minerals were proposed as prospecting guides for submarine hydrothermal vents, which often associate with sulfide ores and metalliferous sediments [7]. However, the direct application of the methods of onshore mercurymetric prospecting to marine conditions is hardly possible due to the presence of a sedimentary cover (which constrains Hg emission from endogenous sources and ore deposits) and a water mass into which the hydrothermal fluids are discharged. Depending on certain sedimentological and oceanological conditions, these factors could significantly modify the localization and intensity of Hg lithochemical dispersion halos above endogenous sources and ore deposits. In addition, unlike other metals that participate in the hydrothermal process (Fe, Mn, Ni, Cu, and Zn) and are utilized in geochemical surveys, Hg migrates with gases, whose behavior upon discharging in bottom waters is different from that of aqueous fluids.

This assumption needed to be tested by studying lithochemical dispersion halos of Hg above submarine fluid vents in recent rifting zones. For this purpose, we studied the distribution of Hg and some other ore elements and the mineral–geochemical features of the Quaternary deposits of the Deryugin Basin in the Sea of Okhotsk, one of the most thoroughly studied marginal sea rift basins.

This basin is typically considered to be a Late Cenozoic rift zone [7, 8] and consists of two tectonic systems: the Deryugin spreading rift system (DSRS [8]; rift trough, [7]) with a sedimentary cover up to 10–13 km thick and the Central–Okhotsk transtensional rift system (COTS [8], rift graben [7]). The axial and western part of DSRS (Fig. 1) contain numerous gas vents, which cause the hydrogen sulfide pollution of the sediments, the intense accumulation of Mo and other trace elements [9], and pervasive diagenetic cementation by gashydrates, carbonates, and enrichment in amorphous iron sulfides [10, 11]. The area within COTS east of DSRS is characterized by the strongest heat flow in the Sea of Okhotsk [8], a highly rugged relief of the acoustic basement dominated by SE-trending linear structures and exposures at the seafloor, massive barite mineralization of Holocene age [12, 13], hydrothermal Fe–Mn crusts [14], and extremely high contents and accumulation rate of Mn and some trace elements (Ba, Zn, and Ni) in both the oxidized and the reduced sediments as compared to other sediments of the Sea of Okhotsk [9, 15, 16].

No direct observations of endogenous sources have ever been conducted in the central part of the Deryugin Basin, and there are only indirect traces of endogenous activity: an elevated heat flow, methane anomalies in the bottom water, and some geophysical data [13, 17, 18]. The fluxes of gas and aqueous metalliferous fluids can be grouped in two types: elision (from sedimentary sequences of the Deryugin trough) and postmagmatic (from interstratal intrusions) [9, 12, 13, 18].

## MATERIALS AND METHODS

Sediment cores were taken by gravity corers and multicorers during cruises of the R/V *Akademik Nesmeyanov* (1993), *Academik Lavrentiev* (1996, 1997, and 2002) [11, 13, 19], and the M/V *Marshal Geolovani* (1999) [17] (Fig. 1).The collecting of the cores, their primary studies, including measurements of the mechanical parameters of the sediments, their water content, magnetic susceptibility, and color, as well as their description and sampling, were conducted in compliance with conventional techniques [11, 17, 19]. Samples for Hg determination were placed into polyethylene pockets, sealed, and stored wet until measurements were taken. Before analysis, the samples were air-dried and ground in an agate mortar. Some samples (core LV28-34-3) were taken from core material, which had been kept in plastic containers in a dry state.

The Hg content was determined by atomic absorption on a PA-915+ analyzer equipped with an RP-91C pyrolitic system (LUMEX, St. Petersburg). The samples were analyzed without preliminary preparation, using standard techniques and GSO 7263-96 and GSO 7183-95 standards. The data were processed by a computer linked with the analyzer.

The contents of Al, Ti, Fe, Mn, and trace elements in sediments were determined by atomic absorption [20, 21] on a Hitachi Limited (180-5) flame analyzer, by atomic emission [22] on a PLASMAQUANT 110 spectral–analytical complex at the Far East Geological Institute, Far East Division, Russian Academy of Sciences, and by INAA [23] using multichannel impulse analyzer and a high-resolution semiconductor detector.

Organic carbon (in some samples) and total sulfur were determined chromatographically on a CARLO ERBA NA-1500 analyzer without preliminary decomposition of the samples. The analysis was based on a instantaneous oxidation of components in oxygen at a temperature of 1050°C, passing the combustion products in a helium flow with accumulation (at 650°C) on a copper catalyst in tin or silver containers. Organic carbon was determined mainly by the Tyurin method in its TsINAO modification [24]. The content of calcium carbonate and amorphous silica were determined by conventional techniques for individual cores [9]. Because of pervasive diagenetic alterations of sediments from the Deryugin Basin, these parameters cannot always be used for the determination of biogenic silica and car-

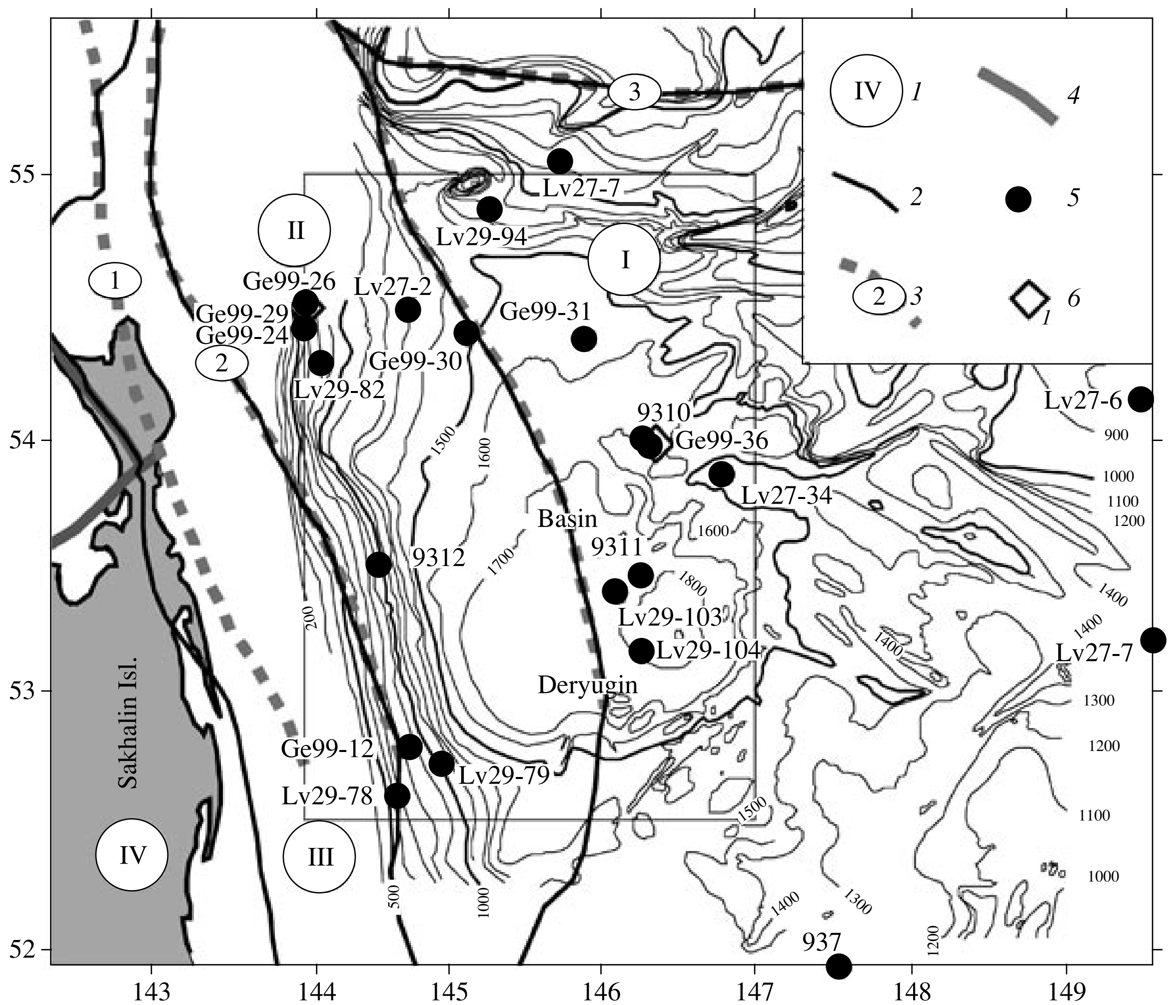


**Fig. 1.** Sampling sites of bottom sediment cores and some structural elements of the Deryugin Basin and Northern Sakhalin. Bottom relief is shown according to [17]. Rectangle outlines fragment shown in Fig. 3. (*1*) Structural–tectonic zones [8]: (I) Central Okhotsk System, (II) Deryugin spreading riftogenic system, (III) Cenozoic Hokkaido–Sakhalin folded system, (IV) Northern Sakhalin Basin; (*2*) boundaries of structures; (*3*) suture zones [(*1*) Eastern Sakhalin, (*2*) Western Deryugin, (*3*) Kashevarov]; (*4*) major faults; (*5*) sampling sites of sediment cores; (6) location of known endogenous sources: (*1*) Obzhirova Flare, (*2*) "Barite Mounds."

bonate. Therefore, biogenic siliceous and carbonate residues were determined mainly by studying microscopic specimens.

The age of the sediments (retrieved in the cores) was taken from previously published dates obtained by different methods (Table 1). The mechanical properties of the sediments were determined using the technique [19]. The composition of samples was determined by semiquantitative analysis of major sediment-forming components in microscopic specimens [9].

Statistical and graphic treatment was conducted by the STATGRAPH and Excel computer programs. Maps of the distribution of elements and the accumulation rates were constructed in a SURFER 8 software package using a "kriging" interpolation.

## COMPOSITION AND STRATIGRAPHY OF UPPER QUATERNARY SEDIMENTS

The composition and stratigraphy of the Upper Quaternary sediments of the Deryugin Basin are typical of the Sea of Okhotsk; therefore, most of the cores can be reliably correlated with well-studied and dated cores on the basis of lithology, physics, and geochemistry of the sediments [11, 17, 19]. Many cores contained only sediments of isotope–oxygen stages 2 and 1 (IOS). The sediments of 2 IOS with an age of 24–12.4 ka are terrigenous pelites and silts with turbidite interlayers (Fig. 2). In cores LV29-103 and LV29-104, these sediments include thick layers of homogeneous unbedded pelites. In the lower part, the sediments acquire a black color owing to amorphous iron sulfides (hydrotroilite). In air, they are oxidized and acquire an olive-gray color similar to that of the upper member. No other significant differences

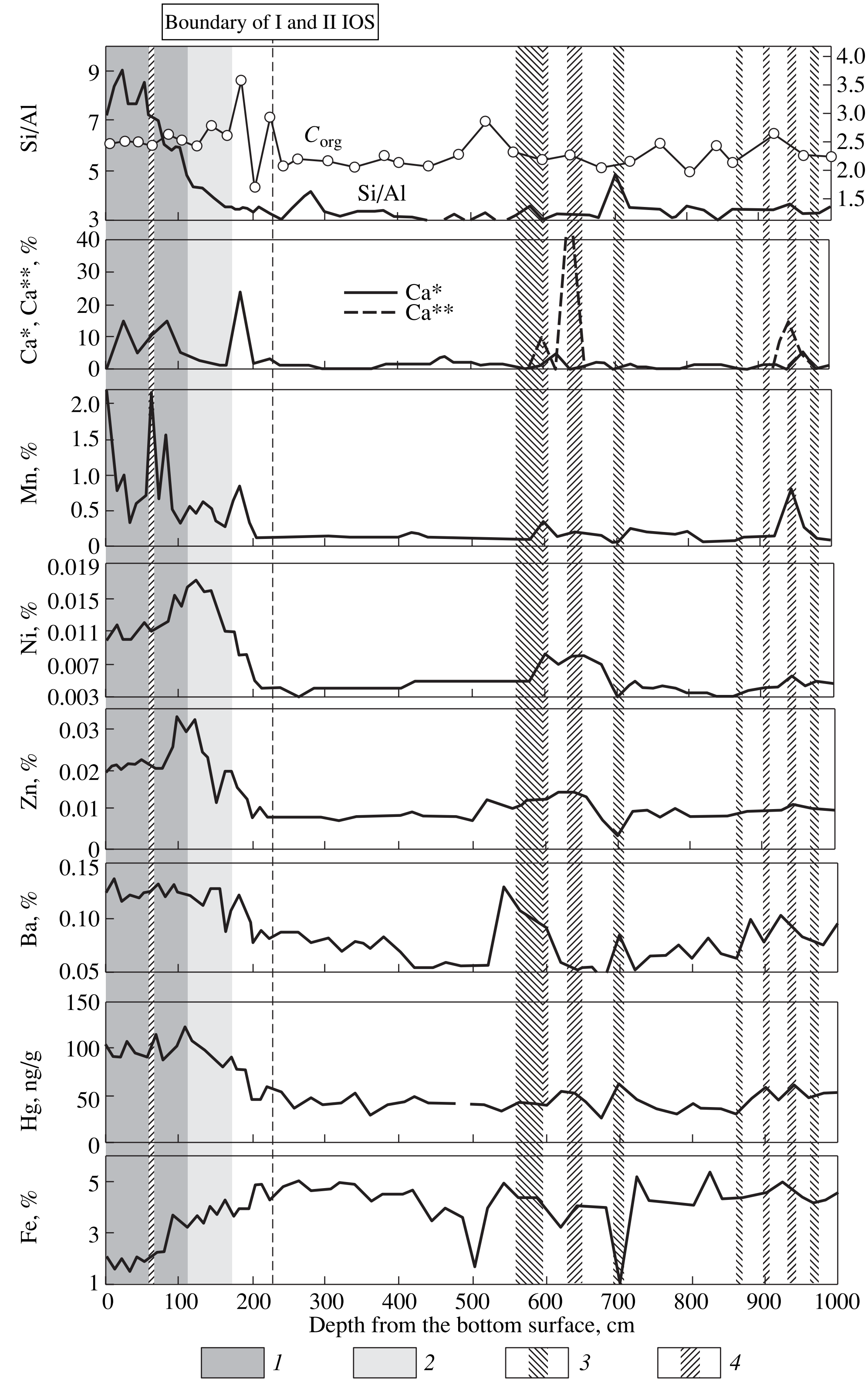


**Fig. 2.** Content of Hg, biogenic components, and some ore elements in the sediments of core Ge99-31-4. Contents of elements are shown based on atomic absorption data; Ca* and Ca** are carbonate contents based on analysis of microscopic specimens: (Ca*) biogenic, (Ca**) authigenic. (*1*–*2*) diatomaceous muds: (*1*) siliceous, (*2*) low-silica; (*3*) sandy turbidite interbeds; (*4*) layers with carbonate nodules or cementation of sediments by carbonate.

**Table 1.** Sampling site coordinates and depths of sediment cores, sedimentation rate (SR), absolute mass (AM)

| Station number | Sea depth, m | Coordinates | | | | Depth of the lower boundary of level*, cm | | Density of dry sediment by horizons, g/cm$^3$ | | | Sedimentation rate by horizons, abs. mass | | | | | | Method of stratigraphic subdivision***, reference |
|---|---|---|---|---|---|---|---|---|---|---|---|---|---|---|---|---|---|
| | | Latitude, N | | Longitude, E | | | | | | | SR, cm/10$^3$ yr | | | AM, g/cm$^2$ 10$^3$ yr | | | |
| | | grad | min | grad | min | Ia | Ib | Ia | Ib | I | Ia | Ib | I | Ia | Ib | I | |
| 937 | 1350 | 52 | 1.50 | 147 | 32.80 | 85 | 104 | 0.27 | 0.48 | 0.34 | 10.6 | 4.2 | 8.3 | 2.9 | 2.0 | 2.8 | m, l [16] |
| 9310 | 1505 | 54 | 0.7 | 146 | 17.0 | – | 3 | – | – | – | – | – | – | – | – | – | m, l |
| 9311 | 1740 | 53 | 30.0 | 146 | 15.8 | 48 | 65 | 0.31** | 0.46** | 0.42** | 6.0 | 3.8 | 5.2 | 2.8 | 1.7 | 2.2 | m, l |
| 9312 | 1010 | 53 | 32.30 | 144 | 33.70 | >680 | – | 0.50 | – | 0.50 | >85 | – | – | >42 | – | – | m, l [16] |
| Ge99-12-4 | 880 | 52 | 51.46 | 144 | 45.58 | 810 | >824 | 0.44 | 0.50 | 0.45 | 103.0 | – | >66 | 45.3 | – | >30 | m, l [17] |
| Ge99-24-2 | 700 | 54 | 26.662 | 144 | 4.517 | 310 | >360 | 0.44** | 0.50** | 0.45** | 38.7 | | >29 | 24.5 | – | >13 | ″ |
| Ge99-26-2 | 700 | 54 | 31.176 | 144 | 5.276 | >582 | – | 0.44** | – | – | >73 | – | – | >32 | – | – | ″ |
| Ge99-29-2 | 700 | 54 | 26.780 | 144 | 4.860 | >26 | – | – | – | – | – | – | – | – | – | – | ″ |
| Ge99-29-3 | 700 | 54 | 26.784 | 144 | 4.765 | 310 | >350 | 0.56 | – | 0.56 | 43.7 | – | >43.7 | 24.5 | – | >24.5 | ″ |
| Ge99-30-3 | 1480 | 54 | 24.576 | 145 | 7.811 | 120 | 290 | 0.37 | 0.46 | 0.42 | 15.0 | 37.8 | 23.2 | 5.6 | 17.4 | 9.7 | ″ |
| Ge99-31-2 | 1600 | 54 | 23.699 | 145 | 52.917 | >44 | – | – | – | – | – | – | – | – | – | – | ″ |
| Ge99-31-4 | 1600 | 54 | 23.492 | 145 | 54.149 | 105 | 196 | 0.53 | 0.63 | 0.58 | 13.1 | 20.2 | 15.7 | 7.0 | 12.7 | 9.1 | ″ |
| Ge99-36-1 | 1520 | 53 | 59.474 | 146 | 19.369 | – | – | – | – | – | – | – | – | – | – | – | ″ |
| Lv27-2-4 | 1305 | 54 | 30.15 | 144 | 45.14 | 330 | 585 | 0.34 | 0.50 | 0.38 | 41.2 | 56.7 | 46.8 | 14.0 | 28.4 | 17.8 | i, p. m. l [16] |
| Lv27-4-4 | 857 | 55 | 3.54 | 145 | 44.16 | – | 11 | 0.84 | 0.84 | 0.84 | 0.9 | 0.9 | 0.9 | 0.8 | 0.8 | 0.8 | m, l [19] |
| Lv27-6-4 | 868 | 54 | 9.87 | 149 | 30.33 | 30 | 170 | 0.63 | 0.71 | 0.67 | 3.7 | 31.1 | 13.6 | 2.4 | 22.1 | 9.1 | ″ |
| Lv27-7-4 | 1140 | 53 | 15.27 | 149 | 35.73 | 10 | 65 | 0.63 | 0.71 | 0.67 | 1.2 | 12.2 | 5.2 | 0.8 | 8.7 | 3.5 | ″ |
| Lv28-34-2 | 1431 | 53 | 52.971 | 146 | 47.499 | 55 | 110 | 0.31** | 0.46** | 0.42** | 6.9 | 12.2 | 8.8 | 2.1 | 5.6 | 3.7 | m, l [13] |
| Lv29-78-2 | 655 | 52 | 40.244 | 144 | 41.187 | 460 | >780 | 0.53 | 0.57 | 0.55 | 57.5 | – | >62 | 30.5 | – | >34 | m, l[17] |
| Lv29-79-2 | 1102 | 52 | 47.477 | 144 | 57.900 | 590 | >800 | 0.47 | 0.53** | 0.50** | 73.7 | – | >64 | 34.7 | – | >32 | ″ |
| Lv29-82-1 | 795 | 54 | 18.15 | 144 | 10.80 | 540 | >790 | 0.53* | 0.53** | 0.53** | 67.5 | – | >55.6 | 35.8 | – | >29.5 | ″ |
| Lv29-94-2 | 1142 | 54 | 52.82 | 145 | 16.55 | – | 12 | – | – | 0.71** | – | – | 1.0 | – | – | 0.7 | ″ |
| Lv29-103-1 | 1746 | 53 | 26.627 | 146 | 5.344 | >45 | – | – | – | – | – | – | – | – | | – | ″ |
| Lv29-103-2 | 1746 | 53 | 26.15 | 146 | 6.05 | 75 | 155 | 0.31 | 0.46 | 0.42 | 9.4 | 17.8 | 12.4 | 2.9 | 8.2 | 5.2 | ″ |
| Lv29-104-2 | 1758 | 53 | 12.850 | 146 | 15.642 | 40 | 90 | 0.31** | 0.46** | 0.42** | 5.0 | 11.1 | 7.2 | 1.5 | 5.1 | 3.0 | ″ |

Notes: (–) data are absent.

* (Ia) 0–8 ka, (Ib) 8–12.4 ka, (I) 0–12.4 ka.

** Average value for given type of sediment [16].

*** (i) isotope–oxygen, (m) paleomagnetic, (p) micropaleontological, (l) lithostratigraphical.

were found between these two types of sediments. Cores 9310 and Ge99-36 from the Barite Mounds area do contain sediments of 2 and 3 IOS, with no sediments of 1 IOS [17, 25].

The sediments of 1 IOS with an age less than 12.4 ka include Holocene and Pleistocene (late-glacial events of the Late Dryassic and Bolling–Allerod) diatomaceous and terrigenous pelites with a high content of biogenic components. In terms of biogenic components, physical properties, and lithology, the 1 IOS sediments can be subdivided into three lithostratigraphic units [9]: diatomaceous, transitional, and foraminiferal, with several characteristic lithological markers. The diatomaceous unit (0–6 ka) is noted for a high content of biogenic silica, which is recorded in the distribution of amorphous silica and the Si/Al ratio, and in the microscopic determinations of diatomaceous remnants [26]. The sediments of the transitional unit (6–8 ka) also contain diatomaceous remnants, whose amount decreases to the bottom of the unit. The foraminiferal unit (8–12.4 ka) has a low content of diatomaceous remnants but high contents of calcium carbonate and organic carbon in the sediments [9, 26]. It includes an Upper Dryassic unit with a low content of biogenic material, which is similar to sediments of 2 IOS [9].

For further considerations, the 1 IOS sediments were subdivided into two lithostratigraphic units. Unit 1a (Table 1) with an age of 0–8 ka corresponds to previously distinguished siliceous and transitional biogenic lithostratigraphic units: its lower boundary was distinguished (from top to bottom) by a decrease in the contents of organic carbon, $CaCO_3$, and magnetic susceptibility, as well as by an increase in biogenic silica. Unit Ib with an age of 12.4–8 ka corresponds to the foraminiferal biogenic unit [6, 26]. During the stratigraphic analysis, the boundary between units 2 and 1 OIS was outlined by an increase in biogenic carbon and the unusual intercalation of sedimentary beds of different color and composition, which correspond to the Bolling–Allerod and Dryas events.

## RESULTS AND DISCUSSION

Analysis of Hg distribution in the surface sediments (Fig. 3, Table 2) makes it possible to distinguish two high-Hg areas: the central part of the basin and the lower part of the continental slope of Sakhalin Island, which is adjacent in the east to areas with known methane vents [13]. In the central part of the basin, anomalous Hg contents in sediments were found near known methane vents in the Barite Mounds area [18], where Hg was also sporadically supplied by aqueous Ba-bearing fluids along faults, as it takes place in a mud volcano [12, 17].

Sediment cores demonstrate several types of Hg distribution. In the upper part of the Sakhalin continental slope, most cores composed of diatomaceous muds have very low and steady contents throught the entire section (Fig. 4). Compositional variations, gashydrates (Fig. 4), carbonate mineralization, and diagenetic alteration exert no significant effect on the Hg content. Its average contents of 15–25 ng/g are close to the background values (11 ng/g) found in the sediments of the Sea of Okhotsk. The exception is core Ge99-29-3, whose lower part demonstrates sharply variable and anomalous contents. The highest Hg contents were found in sediments located beneath the gas-hydrate layer, though its very high contents were also noted in some units above it. In general, this core has a higher Hg content than those in the adjacent cores.

The central part of the depression shows a significant increase in the Hg concentration in the Holocene deposits and especially in the diatomaceous mud from the upper unit with an age of 0–8 ka (Figs. 2, 4). The average Hg contents in these units show wide variations (Figs. 3b, 3c). As in surface sediments, there are two zones with high Hg contents: in the eastern and western parts. The underlying Upper Pleistocene deposits have a significantly lower Hg content at narrow variations, averaging 35–40 ng/g (Fig. 4). The significant variations in Hg content found in some cores from the Upper Pleistocene deposits are presumably caused by compositional variations, in particular, the presence of sandy turbidite intercalations (Fig. 2).

In the Upper Pleistocene sediments, elevated and anomalous Hg contents were found only in cores Ge99-36-1 and 9310 from the Barite Mounds area. There are no Holocene sediments. The Upper Pleistocene sediments of 2 and 3 isotope–oxygen stages differ in widely varying and increased (in core Ge99-36-1) or anomalous (core 9310) Hg contents (Fig. 4). Sediments from these two cores differ in the presence of authigenic barite and carbonate mineralization, which is pronounced most clearly in core 9310 [25].

To estimate the Hg distribution in sediments, the occurrence frequency of its contents was determined in the Holocene and Upper Pleistocene sediments using the technique previously proposed in [9]. The frequency curve allowed us to distinguish samples with close Hg content within the range of 30–100 ng/g (average content of 65 ng/g), including ~65% of the analyses, with this value assumed, then, as the background. This value is close to the range of 10–100 ng/g found for the Sea of Okhotsk [3] and to the average content in sediments from the near-Kurile part of the Sea of Okhotsk but is significantly higher than the local background level (11 ng/g) for sediments from the Sakhalin shelf [27] and, for example, the average value for sediments from the Baltic Sea (20 ng/g) and red deep-water clays (25 ng/g) from the western part of the Pacific Ocean [6].

The accumulation rate of excess Hg masses ($S$, g/cm$^2$ per thousand years) for the Holocene and its discrete stages was calculated using data on the sedimentation rates (Table 1) and average contents (Table 2) by the formula

$$S = (C - C_f) \times R_m/100,$$

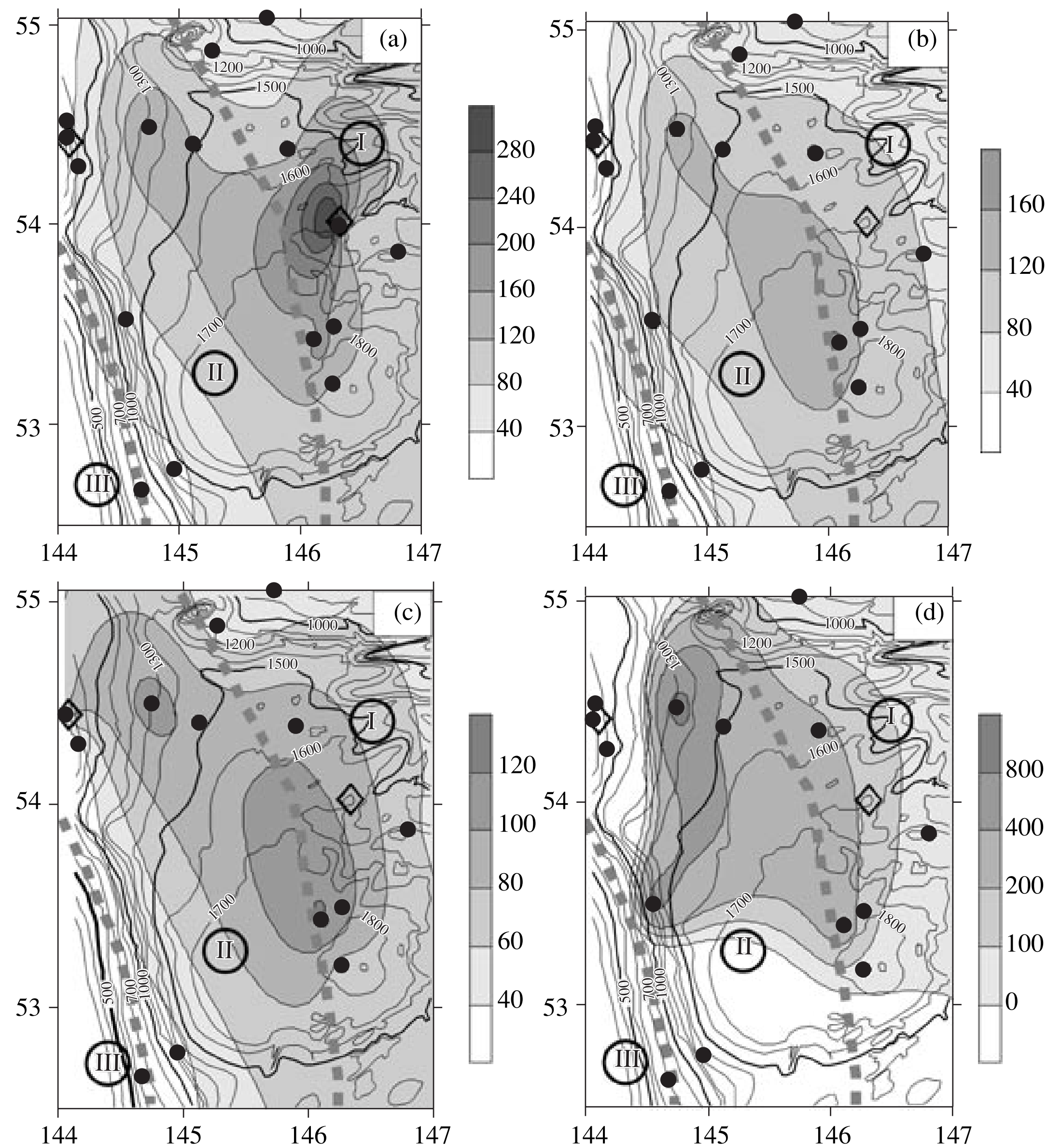


**Fig. 3.** Maps of the contents and accumulation rates of excess Hg in the Deryugin Basin. (a, b, c shows the content of Hg (ng/g): (a) surface sediments, (b) average contents for sediments with an age of 0–8 ka, (c) average contents for sediments with an age of 0–12.4 ka; (d) accumulation rates of excess Hg for 0–2 ka. Other symbols are shown in Fig. 1.

where $R_m$ is the absolute mass (g/cm$^2$ 10$^3$ yr), $C$ is the average Hg content (ng/g), and $C_f$ is the average background content of Hg (65 ng/g).

The map constructed for the Hg accumulation rate (Fig. 3d) reflects, in the general form, its distribution in the sediments shown in the abundance maps (Figs. 3a, 3b, 3c). Unlike the average Hg contents, the highest accumulation rate of its excess masses over the past 8 ka were noted in the western part of the basin.

The data presented above on the Hg distribution and the calculation of the accumulation rates of its “excess” masses allow a simpler interpretation of the anomalous and sharply contrasting Hg contents in cores Ge99-29-3 and 9310. These cores were taken in the areas with known endogenous activity, which is marked by acoustic anomalies in the water column, elevated methane contents in the bottom waters, and the results of visual observations and sonar survey [13]. For example, water column at station Ge99–29 demonstrate a sharply contrasting anomaly of methane contents [11], which was not found at adjacent stations (Fig. 6). Elevated methane contents were later found in bottom waters near station 9310 in the Barite Mounds area [25].

The elevated and anomalous Hg contents in these cores could be regarded as a result of the passage of endogenous aqueous or gas fluids through sediments. A similar “infiltration” type of accumulation of Hg and other metals (Zn, Ba, Mn, Cu, and Pb) was found, for

**Table 2.** Content and accumulation rate of Hg in the cores from the Deryugin Basin

| Core numbers | Hg content, ng/g* | | | | | Accumulation rate of "excess" Hg, ng/cm$^2$ per 1000 yr for period | |
|---|---|---|---|---|---|---|---|
| | Floor surface | Average by column | Level Ia | Level Ib | Level I | 0–8 | 0–12.4 |
| 937 | 132 | 88 | 113 | 70 | 104 | 138 | 110 |
| 9310 | 371 | 256 | – | – | – | – | – |
| 9311 | 150 | 59 | 114 | 100 | 111 | 135 | 100 |
| 9312 | 67 | 76 | 76 | – | 76 | >480 | – |
| Ge99-12-4 | 55 | 88 | – | – | – | – | – |
| Ge99-24-2 | 17 | 14 | 14 | 16.5 | 15 | –868 | <–650 |
| Ge99-26-2 | 26 | 23 | 23 | – | – | <–1340 | – |
| Ge99-29-3 | 74 | 88 | 76 | 271 | 88 | 277 | >320 |
| Ge99-29-2 | 69 | 28 | 28 | – | – | – | – |
| Ge99-30-3 | 118 | 65 | 116 | 84 | 97 | 284 | 307 |
| Ge99-31-2 | 98 | 109 | 109 | – | – | – | – |
| Ge99-31-4 | 106 | 56 | 97 | 93 | 96 | 225 | 279 |
| Ge99-36-1 | 100 | 98 | – | – | – | – | – |
| Lv27-2-4 | 158 | 109 | 135 | 70 | 109 | 980 | 783 |
| Lv27-4-4 | 48 | 48 | 48 | 48 | 48 | –14 | –14 |
| Lv27-6-4 | 49 | 34 | 41 | 19 | 34 | –58 | –285 |
| Lv27-7-4 | 50 | 71 | 50 | 50 | 50 | –52 | –228 |
| Lv28-34-2 | 104 | 50 | 78 | 39 | 63 | 29 | –9 |
| Lv29-78-2 | 20 | 21 | 19 | 24 | 21 | –1402 | <–1510 |
| Lv29-79-2 | 31 | 35 | 34 | 38 | 35 | –1075 | <–960 |
| Lv29-82-1 | 45 | 32 | 31 | 34 | 32 | –1217 | <–976 |
| Lv29-94-2 | 51 | 44 | – | – | 51 | –10 | –10 |
| Lv29-103-1 | 140 | 133 | – | – | – | – | – |
| Lv29-103-2 | 197 | 65 | 168 | 96 | 123 | 300 | 301 |
| Lv29-104-2 | 114 | 38 | 104 | 50 | 72 | 58 | 20 |

* (–) not determined.

example, above magmatogenic hydrothermal vents overlain by sediments in the northern part of the Mid-Atlantic ridge [5]. Anomalous and elevated contents of these elements and high accumulation rates are typical of the Barite Mounds area, which was sampled by core 9310 [9, 15]. It is believed that massive barite chimneys covering a giant area and having a height of up to 8 m were formed by the infiltration of Ba-bearing fluids along faults in the sedimentary cover [17]. Some researchers believe that these processes are similar to mud volcanism [12], which is typically characterized by a sharp increase in gas and fluid fluxes in short-term periods of their eruptive activity. During dormant periods, the fluid fluxes were minimal. For example, active eruptions of mud volcanoes at Sakhalin Island occurred with a periodicity of 5–20 yr [28]. During eruptions and some time after them, a sharp increase was detected in the Hg content in the gases, in the fluid temperature, and in the contents of Ba and B in them, as well as in the contents of Mn and some trace elements in the mud-volcano breccia [28, 29]. The Daginsk mud volcanoes located within the Northern Sakhalin Sedimentary Basin, the closest to our study area, are associated with hydrothermal vents with a temperature of up to 55°C [30].

Based on the typical generation depth of mud volcano chambers equal to 2–3 km [28] and on calculations with geothermal gradients [31], we suggest that the primary temperature of hydrothermal vents in the Barite Mounds area should be no less than 140°C. The temperature can be even higher owing to postmagmatic processes related to the emplacement of intraformational intrusions [18]. When passing through the sedimentary cover, even during periods of active eruptions, fluids cool, and most ore elements are precipitated from them on geochemical barriers in the sedimentary cover. The decrepitation temperature of the spherulitic barites

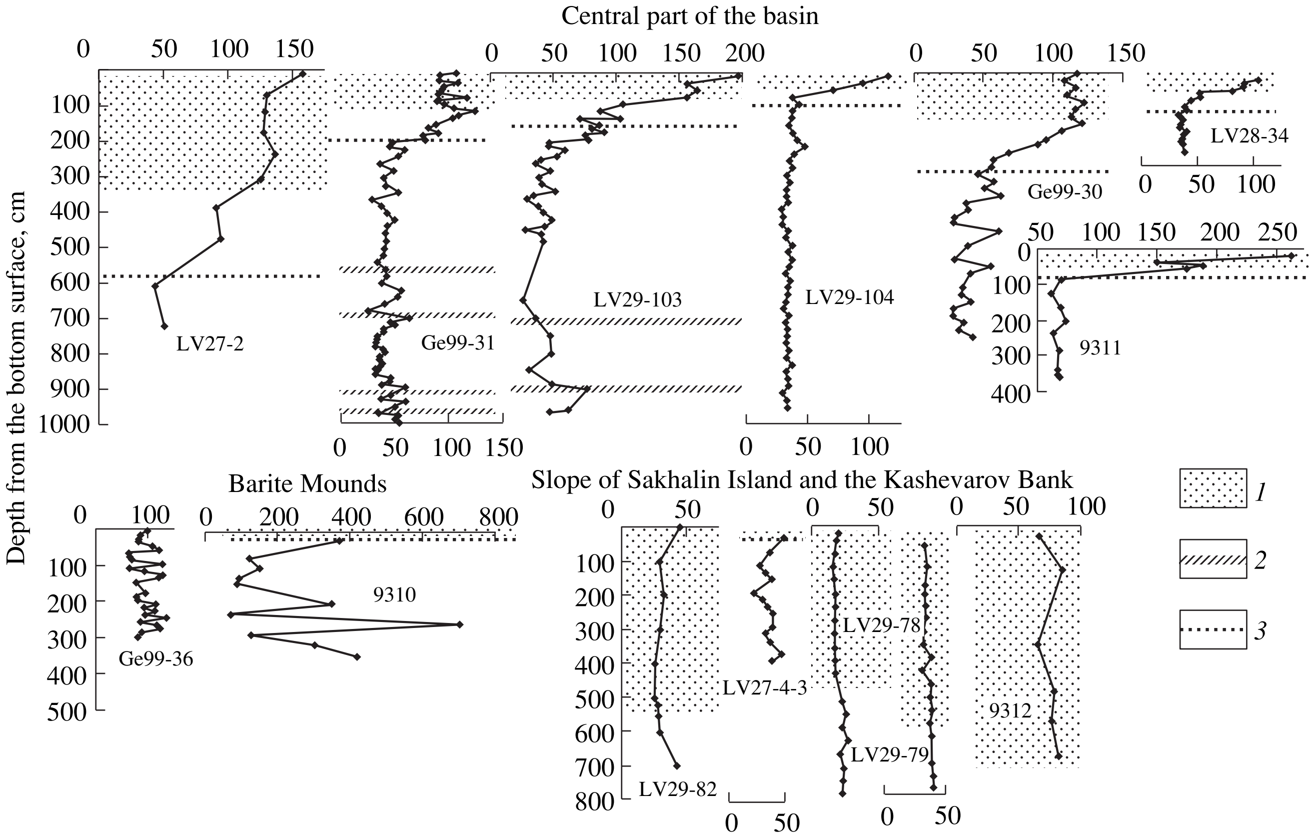


**Fig. 4.** Hg distribution (ng/g) in cores of bottom sediments from three areas and elements of lithostratigraphic subdivision. (*1*) Diatomaceous siliceous and weakly siliceous mud from level Ia (0–8 ka); (*2*) sandy turbidite interbeds; (*3*) boundary between 1 and 2 isotope–oxygen stages.

was ~45°C [12]. The following lines of evidence testify that other metals were also supplied with these aqueous solutions: (1) the formation of hydrothermal Fe–Mn crusts at the surface of the barite chimneys and at adjacent rises; (2) accumulation of Mn metalliferous sediments in the adjacent part of the basin and the enrichment of the Holocene deposits in Fe, Ni, Cu, and Pb; and (3) mineralogical finds of ore sulfides and manganese carbonates among barites and in the basin sediments.

The Sakhalin slope, sampled by core Ge99-29-3, includes only methane vents with no aforementioned traces of the infiltration of hydrothermal fluids. Methane is believed to rise along faults from oil–gas reservoirs and destabilized gas-hydrates [13]. Methane anomalies in the bottom waters are associated with higher Hg contents [27], which can be explained by gas fluxes from oil–gas reservoirs. Many of them are localized in the continental spreading zones (which occur in our study area) and have very high Hg contents [3]. To reveal the characteristics of the infiltration accumulation of Hg under such conditions, it is expedient to consider the composition of sediments and their diagenetic alterations caused by gas fluxes. High Hg contents were found not only in the lower part of core Ge99-29-3 (Fig. 6), where ascending gases can be accumulated beneath the gas-hydrate layer, but also in its upper two-meter part (55 ng/g). Adjacent cores Ge99-24 and Ge99-26 (Fig. 4) have lower Hg contents (15 and 23 ng/g, respectively). Moreover, very low Hg contents (21 ng/g) were found in samples that were taken by a multicorer at station Ge99-29 (Ge99-29-2), 200 meters east of the sampling location, and had an undisturbed top layer; there are also outbursts (Fig. 5) probably caused by an adjacent gas vent.

At total elevated (relative to those in adjacent cores) Hg contents in core Ge99-29-3, a sharp increase in the Hg content was found beneath the gas-hydrate bed (which is a partial fluid trap) and above it, in the 200–270 cm layer, which also has high contents of some other elements (Fig. 6). The element spectrum (S, Fe, Mo, and Sb) and microscopic study of the transparent specimens [32] indicate that high contents of elements in this interval are controlled by the amount of dispersed iron sulfides. Sulfide globules up to a few microns in size and their aggregates up to tens of microns fill cavities in diatom skeletons, partially cementing sediment. Iron sulfides are presumably the main Hg carriers, which is typical of marine sediments [3]. Diagenetic units cemented by carbonates or sulfides

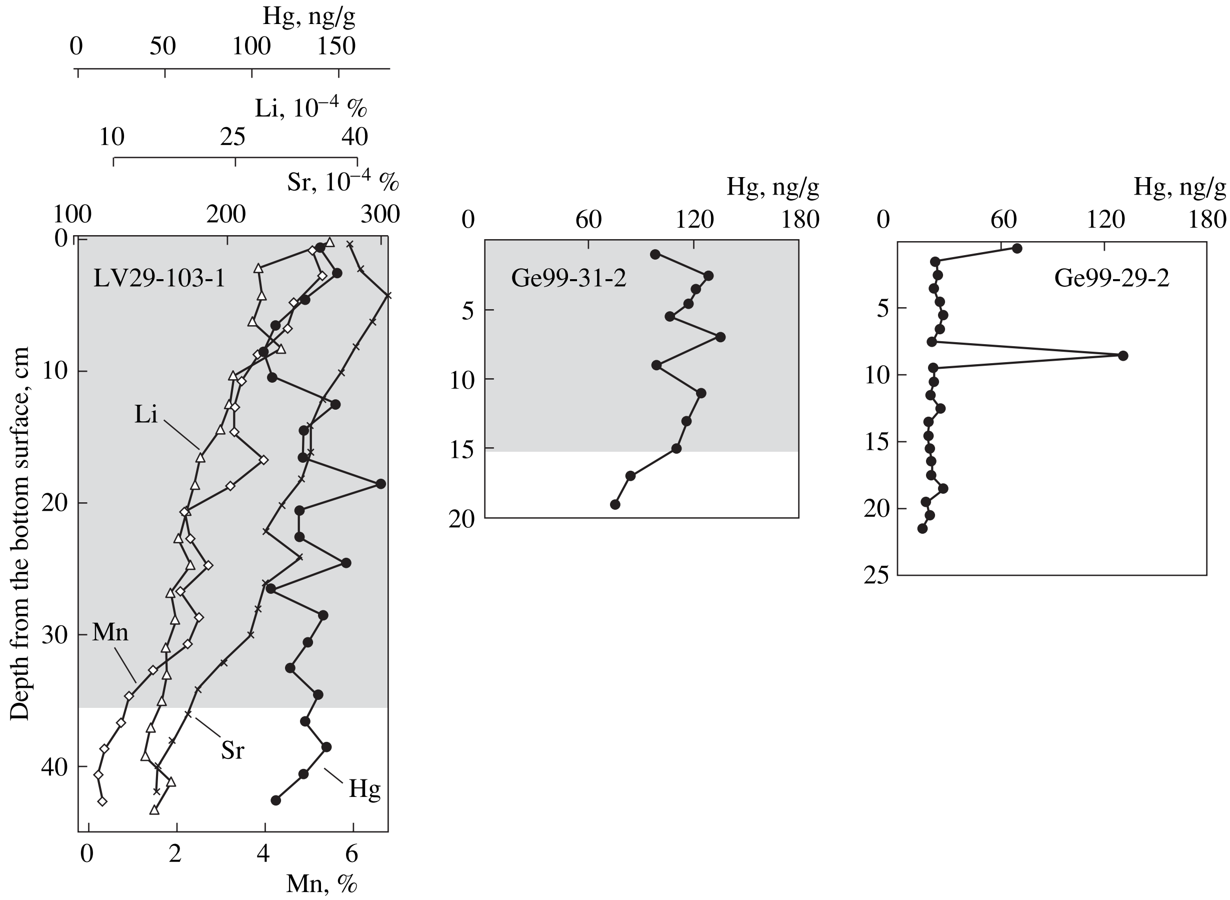


**Fig. 5.** Hg contents in the surface sedimentary bed (ng/g) in the Deryugin Basin obtained on monoliths by multicorer. Gray color shows the oxidized sedimentary bed, the contents of Mn, Sr, and Li that enrich oxidized sediments are shown for column LV29-103-1.

were found in many cores from the slope of Sakhalin [10, 11, 33]. Their formation is thought to have been related to biochemical and physicochemical processes at barriers in contact between marine and interstitial waters, in the presence of methane fluxes from the sedimentary cover. These units can also be distinguished using the mechanical properties of their sediments, which makes it possible to trace them over a significant distance by high-frequency acoustic sounding [11]. In core Ge99-29-3, such a layer can also be distinguished owing to its low water content (Fig. 6) and an elevated density.

Sediments lying beneath the gas-hydrate layer and sharply enriched in Hg also have elevated Se contents. The sediments were analyzed for many elements, including Al, As, Ba, Br, Ca, Co, Cr, Cs, Cu, Hf, K, Ni, Na, Rb, Si, Sr, Sc, Ta, Ti, Th, U, Zn, Zr, REE, and others. In the sediments overlaying the gas-hydrate layer, Se correlates with Fe, though its contents are significantly lower than in sediments beneath the gas-hydrate layer.

Our data indicate that the presence of gas hydrates in sediments is not a decisive factor controlling high Hg contents. In core Ge99-24-2, a significantly thicker gas-hydrate layer was penetrated at the same depth as in core Ge99-29-3; the sediments demonstrate the same extensive diagenetic alterations related to the anaerobic oxidation of methane by seawater sulfate, in particular, a large amount of carbonate nodules, $H_2S$ pollution, and similar hydrochemical characteristics of mud waters [17]. However, the Hg contents are there at a minimum and lower than the background ones. This indicates that anomalous Hg contents were produced under these conditions mainly by a gas vent. In core Ge99-24-2 with a well-pronounced gas-hydrate layer (Fig. 4), which served as a fluid trap, the methane source is presumably the gas-hydrate bed itself. In core Ge99-29-3, this bed was almost completely decomposed (though serves as a partial fluid trap, judging from the Hg content beneath it) and is penetrated by deep-seated gases. As was mentioned above, the latter came mainly from oil–gas reservoirs and are enriched in Hg. In this case, the absence of Hg in the gas-hydrate beds may be indicative of a different source than a flux of deep-seated gases along faults. The low S content in the sediments of the gas-hydrate layer, similar to those in the surface sediments (Fig. 6), suggests that these sediments were conserved by gas hydrates at the floor surface simultaneously with sedimentation and prior to sulfate reduction. In this case, the Hg-bearing gases forming the main methane anomalies in the water column could be unrelated to gas-hydrates and have another deeper seated origin. Judging by the carbon isotope composition of carbonate nodules from the Obzhirova Flare methane vent area, these gases originate from oil–gas reservoirs [34].

The maps constructed for Hg contents in the Holocene sediments and the accumulation rates of Hg excess masses indicate the intense accumulation of Hg only partially spatially related to endogenous sources over most of the basin. Similarly to those in midocean ridge areas [5], this type of Hg accumulations can be ascribed to a *plume*. This zone is characterized by an even Hg distribution throughout the Upper Quaternary sediments. The Holocene sediments in general and the diatomaceous muds of the upper lithological unit in particular show a significant Hg enrichment. The underlying sediments have background contents, weakly varying over the area. The exceptions are cores Ge99-36 and 9310 in the Barite Mounds areas. As was considered above, core 9310 has anomalously high Hg contents, which can be ascribed to the infiltration type. In core Ge99-36, its contents are significantly higher than the background contents for clay muds of other cores, but are significantly lower that those in core 9310, with weak variations throughout the section.

The Hg distribution in almost all cores from the central part of the basin, the variations in the average Hg contents in the Holocene sediments and in the accumulation rates are close to those for Mn and some trace elements (Ba, Zn, Ni, and Cu). This is well illustrated by their distribution in the cores (Fig. 2), on the diagrams (Fig. 7), as well as by the comparison of the distribution maps and accumulation rates of Hg (Fig. 3) and other elements [9]. The analysis of distribution maps of Mn and Hg also showed a correlation, though certain data on the distribution in individual cores (Figs. 2, 5) show no correlation. This is presumably related to the intense postsedimentation redistribution of Mn with its accumulation in the oxidized bed (Fig. 5) or individual "interbeds" of reduced sediments bearing diagenetic carbonates and sulfides (Fig. 2). The correlation between Hg and organic matter, which is indicative of atmospheric Hg flux into the basin, is absent from both the diatomaceous muds and the terrigenous part of the section (Fig. 7).

The model of accumulation from water plumes above low-temperature hydrothermal vents sporadically reactivated in the Barite Mounds area was previously proposed for Mn [9, 16]. Such a deposition of Mn hydroxides on the surface of particles precipitating through a hydrothermal plume was revealed, for example, in a similar geological environment in the southern part of the Okinawa trough [35]. It was demonstrated

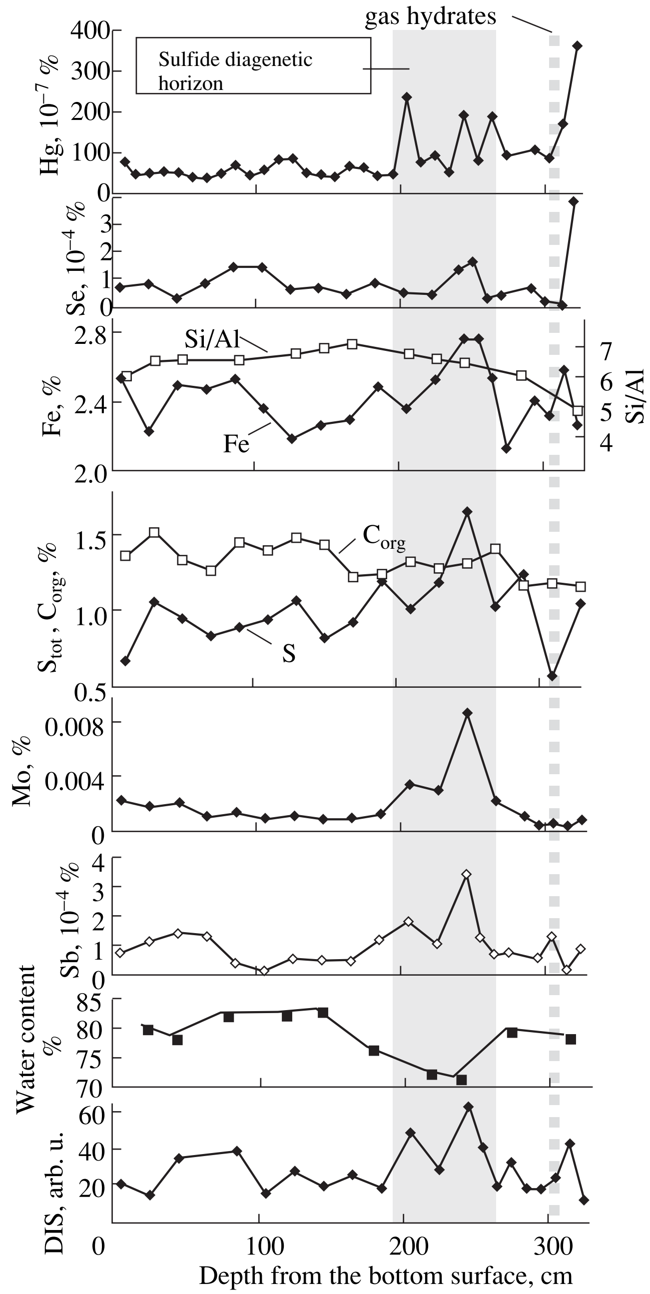


**Fig. 6.** Contents of Hg and some lithological–geochemical characteristics of sediments from core Ge99-29-3. The content of diagenetic iron sulfides (DIS) was determined in microscopic specimens by the degree of coverage by black opaque minerals in the vision field of the microscope [32]. The figure illustrates the enrichment of sediments beneath the gas-hydrate layer in Hg and Se, and of the sulfide diagenetic layer in Fe, S, Mo, Hg, Sb, and diagenetic sulfides; as well as its decreased water content (porosity).

that large plumes above endogenous sources in the Deryugin Basin could be formed only in a stratified water column formed during interglacial periods [9]. Intense water mixing during glaciations prevented stratification [36] and the formation of abundant water plumes above

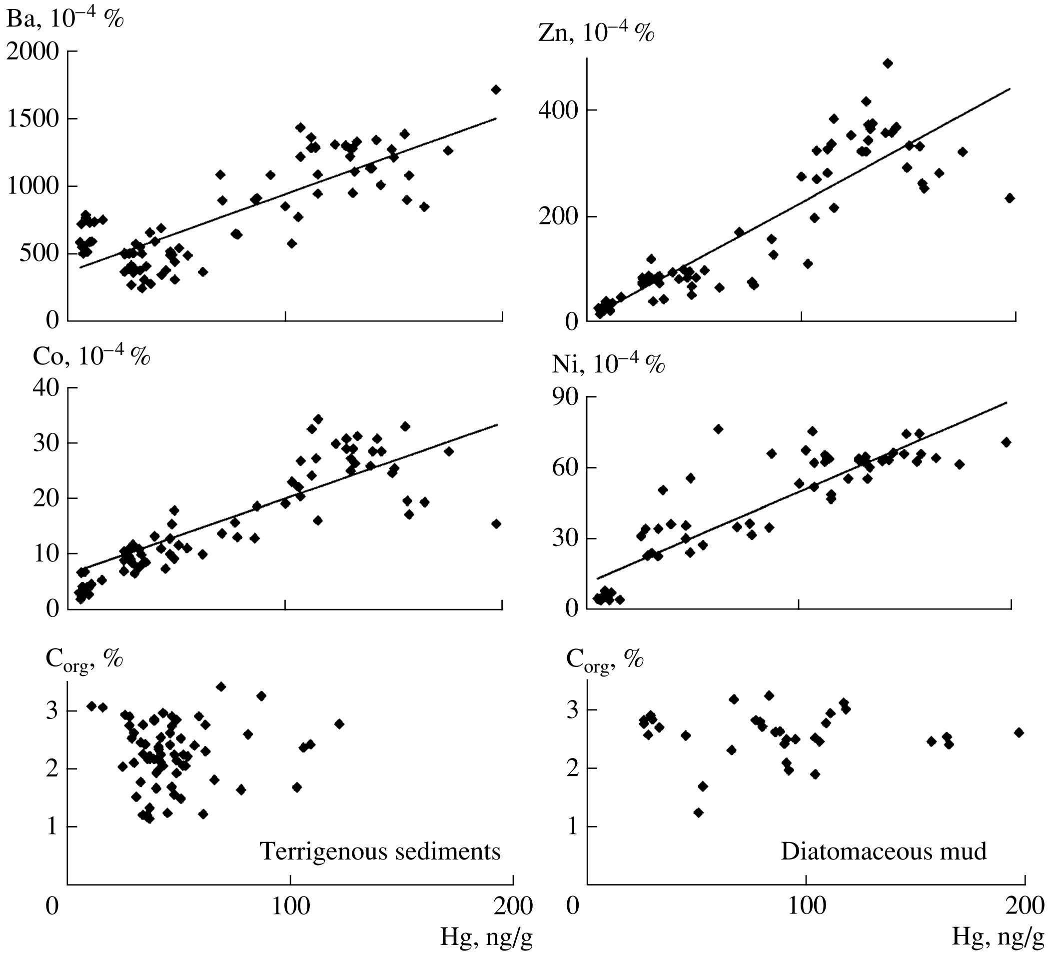


**Fig. 7.** Variations in the Hg contents (ng/g) versus Zn, Ni, Co, Ba, and organic matter from sediments of the Deryugin Basin.

endogenous sources. Intense Mn and Hg (according to our data) accumulation during that time [16] could occur only near hydrothermal vents, as was mentioned above for core Ge99-36.

More complex mechanisms are inferred for the intense accumulation of Ba and some trace elements in the central part of the basin. These are the coprecipitation of trace elements from seawaters by Mn and Fe hydroxides (a process most typical of Ni) and the coprecipitation from water plumes with biogenic matter. The coprecipitation is thought to be the leading mechanism in the precipitation of Ba and Zn from seawater [9]; these elements could be selectively accumulated in carbonate plankton depending on the hydrochemical state of water [37, 38]. In the Sea of Okhotsk, biogenic carbonate is almost not preserved in sediments (unlike silica), though their production rates were approximately similar, judging from data on sedimentation traps [39]. The metals precipitated with biogenic carbonate after the dissolution of carbonate matrix could be accumulated in the sediments, and variations of their contents will be similar to those of biogenic silica.

We believe that most of the excess Hg in the sediments of the Deryugin Basin is accumulated in a similar way. Cores from the central part of the basin (Fig. 2, 4) show a good correlation between Hg and biogenic silica: the most Hg-enriched rocks are diatomaceous muds, though similar muds at the Sakhalin slope have the lowest Hg contents (Fig. 4). Unlike Mn, Ba, and some other elements (Zn and Ni), whose excess masses are most rapidly accumulated in the central part of the Deryugin Basin, Hg could be supplied from the Earth's crust not only from subaqueous water vents but also together with gases. As was established for the northeastern Sakhalin slope and Piip Volcano in the Bering Sea [40], gas bubbles rise from the floor at depths of 400–700 m to the sea surface. This maintains elevated Hg contents not only in the bottom waters but also over the entire water column, up to the photosynthesis layer, where its biosedimentation precipitation could be maximal. This presumably explains the different location of zones of the intense accumulation of Hg and other heavy metals in diatomaceous muds of the Deryugin Basin. Zones of intense accumulation of excess Ba, Zn, and Ni are localized in the Barite Mounds area and northwest of them [9]. Intense Hg accumulation occurs not only in this area but also at the lower part of the Sakhalin slope (Fig. 3 d). The maximum accumulation rates of excess Hg were detected at the Sakhalin slope, which presumably results from Hg supply from gas vents. However, diatomaceous muds in the gas vent area demonstrate low Hg contents, even below the background level. The reasons for this distribution can be different. For example, this can be explained by the precipitation of biogenic material formed above gas vents in the deeper seated parts of the basin or by specific hydrochemical conditions of the bottom or interstitial waters preventing Hg accumulation in sediments. In addition, the absence of intense Hg accumulation in the Obzhirova Flare gas vent area could be explained by the young age of these vents, which is supposed by some researchers [34]. In any case, this phenomenon requires additional study.

The comparison of the maps (Fig. 3) demonstrates that areas with high Hg contents and especially, with high accumulation rates of Hg excess mass over the past 8 ka coincide with the spreading riftogenic structure. This coincidence is explained by the location of gas and hydrothermal vents in the peripheral parts of the structure, as well as by uncompensated subsidence within the latter, which determined the formation of a deep, relatively isolated basin. The repeatedly developing vertical water stratification in this basin facilitates the formation of abundant plumes with specific hydrochemical conditions in the bottom waters and "plume" anomalies in the bottom sediments. This confirms the earlier conclusion that oceanic and intracontinental riftogenic structures contain elevated Hg concentrations [3, 6] as fluid-conducting zones that ensure the vertical migration of mantle fluids. However, Hg supply from hydrothermal and gas vents in subaqueous conditions does not always lead to the formation of abundant lithochemical Hg dispersion halos similar to those in the Okinawa trough [6] or found in the central part of the Deryugin Basin (our data). Favorable oceanological (paleoceanological) conditions are required. At the same time, our data showed that local Hg anomalies could be formed in sediments immediately at the place of endogenous vents (gas and hydrothermal). In general, the mapping of lithochemical Hg dispersion halos could be applied to prospecting of endogenous vents on the seafloor. To reveal an anomaly related to hydrothermal vents, which are promising for sulfide and barite deposits, additional geochemical signatures, such as increased contents of other elements (Fe, Mn, Au, Ag, Ba, Zn, and Ni) in sediments, must be used [5, 6, 9].

The aforesaid can be summarized as follows.

Our study showed that elevated and anomalous Hg contents in the Holocene sediments of the Deryugin Basin and adjacent areas of the Sea of Okhotsk are related to an active riftogenic structure and individual fluid vents within it. Hg fluxes from gas and low-temperature hydrothermal vents associated with favorable oceanological conditions in the Holocene caused anomalous and high Hg contents in the sediments. Anomalous and elevated Hg contents in the sediments can be accumulated in two main ways: (1) due to infiltration of hydrothermal or gas fluids from sedimentary cover and (2) precipitation from water plumes with specific hydrochemical conditions forming above endogenous vents.

Infiltration Hg anomalies were found in the area of reliably identified gas vents at the northeastern Sakhalin slope, where elevated Hg contents are related mainly to the accumulation of ascending gases beneath the gas-hydrate bed, and Hg associates only with Se and in the area of the inferred sporadic activation of low-temperature hydrothermal vents in the central part of the Deryugin Basin, which contains massive barite chimney, hydrothermal Fe–Mn crusts, and anomalously high Mn, Ba, Zn, and Ni contents in sediments.

It is possible that Hg precipitates from water plumes mainly by means of biosedimentation. If plumes are formed by low-temperature hydrothermal vents, the Hg anomalies in the sediments are associated with anomalous contents of Ba, Mn, Zn, Ni, and Cu; and gas vents produce only Hg anomalies. Hg anomalies in bottom sediments above gas vents bear less information on the localization of these sources than those above hydrothermal vents. The use of lithochemical Hg dispersion halos of the plume type for prospecting of submarine hydrothermal and gas vents requires incorporation of oceanological conditions. In nonstratified water columns with intense vertical exchange, as in the Deryugin Basin during glaciations, no water plumes are formed, while Hg is scattered giving rise to increased contents only in the vicinity of vents.

## CONCLUSIONS

Anomalously high and high Hg contents in the Quaternary sediments of the Deryugin Basin are produced by Hg fluxes from low-temperature hydrothermal or cold gas vents, which are localized along faults cutting across or bounding riftogenic spreading structure.

Lithochemical Hg dispersion halos in the Quaternary sediments can be used for the identifying and mapping of endogenous vents of different genesis, in combination with other geochemical, geophysical, and mineralogical evidence. The most informative halos are of an infiltration dispersion nature, which are formed by the passage of fluids through the sedimentary cover. Plume Hg dispersion haloes are generated in sediments at a significant distance from endogenous sources and only in favorable physicochemical and oceanological conditions. Their study could be useful for paleooceanological investigations, in particular, for the reconstruction of the vertical stratification of the water column.

## ACKNOWLEDGMENTS

This work was conducted within the framework of the Russian–German COMEX project and was financially supported by the Russian Foundation for Basic Research (project no. 05-05-65217a). We are grateful to N. Biebow, R.G. Kulinich, D. Nurnberg, R. Tiedemann, S.A. Gorbarenko, A.I. Obzhirov, A.N. Derkachev, and A.I. Botsul for help with expedition works, and to V.I. Kiselev and G.A. Bakhareva for help in analytical works.

## REFERENCES

1. W. P. Fitzgerald and R. P. Mason, "The Global Mercury Cycles: Oceanic and Anthropogenic Aspects," in *Global and Regional Mercury Cycles: Sources, Fluxes and Mass Balance*, Ed. by W. Baeyens, R. Ebinghaus, and O. Vasiliev, (Kluver, Dordrecht, 1996), vol. 1, pp. 85–108.
2. A. P. Dastoor and Y. Larocque, "Global Circulation of Atmospheric Mercury: a Modeling Study," Atmos. Environ. **38**, 147–161 (2004).
3. N. A. Ozerova, *Mercury and Endogenous Ore Formation* (Nauka, Moscow, 1986) [in Russian].
4. A. A. Saukov, N. Kh. Aidin'yan, and N. A. Ozerova, *Sketches of the Geochemistry of Mercury* (Nauka, Moscow, 1972) [in Russian].
5. G. A. Cherkashev, Extended Abstracts of Doctoral Dissertation (Moscow, 2004) [in Russian].
6. Z. Yiyang and Y. Mingcai, "Mercury Anomaly in the Okinawa Trough Sediments—An Indicator of Modern Seafloor Hydrothermal Activity," Chin. J. Chem. **14**, 33–39 (1995).
7. V. V. Kharakhinov, Extended Abstracts of Doctoral Dissertation (Vladivostok, 1998) [in Russian].
8. G. Varnavskii, A. E. Zharov, G. L. Kirillova, et al., *Geology and the Oil and Gas Potential of the Okhotsk–Shantarsk Sedimentary Basin* (DVO RAN, Vladivostok, 2002) [in Russian].
9. A. S. Astakhov, S. A. Gorbarenko, G. A. Bakhareva, et al., " Distribution and Accumulation Rate of Ore Elements in the Holocene and Late Glacial Sediments of the Deryugin Basin, Sea of Okhotsk," Litol. Polezn. Iskop., No. 2, 115–132 (2005) [Lithol. Miner. Resour. **40**, 97–113 (2005)].
10. N. V. Astakhova, A. I. Obzhirov, A. S. Astakhov, and S. A. Gorbarenko, "Authigenic Carbonates in Gas Anomaly Zones of Marginal Seas of Eastern Asia," Tikhookean. Geol., No. 4, 34–40 (1993) [in Russian].
11. "Cruise Report: KOMEX. RV Akademik M.A. Lavrentiev Cruise 29, Leg 1 and Leg 2," Ed. by N.Biebow, R.Kulinich, and B.Baranov, GEOMAR Report **110**, 2003.
12. N. V. Astakhova, "Hydrothermal Barite in the Sea of Okhotsk," Resour. Geol., No. 17, 169–172 (1993).
13. "Cruise Reports: KOMEX I and II. RV Professor Gagarinsky. Cruise 22, RV Akademik Lavrentyev Cruise 28," Ed. by N. Biebow and E. Hutten, GEOMAR Report **82**, 1999.
14. N. V. Astakhova and V. V. Sattarova, "Geochemistry of Iron–Manganese Nodules in the Central Part of the Sea of Okhotsk," Vulkanol. Seismol., No. 3, 29–33 (2005) [in Russian].
15. P. L. Bezrukov, "Bottom Sediments of the Sea of Okhotsk," Tr. Inst. Okeanol. Akad. Nauk SSSR **32**, 15–97 (1960) [in Russian].
16. A. S. Astakhov, S. A. Gorbarenko, N. G. Vashchenkova, and Yu. G. Volokhin, "Distribution and Rates of Manganese Accumulation in the Botom Sediments of the Sea of Okhotsk," Tikhookean. Geol. **19** (5), 47–60 (2000) [in Russian].
17. "Cruise Reports: KOMEX V and VI. RV Professor Gagarinsky Cruise 26, MV Marshal Gelovany Cruise 1," Ed. by N. Biebow, T. Ludmann, B. Karp, and R. Kulinich, GEOMAR Report **88**, 2000.
18. R. G. Kulinich and A. I. Obzhirov, "Barite–Carbonate Mineralization, Methane Anomaly and Geophysical Fields in the Deryugin Depression, Sea of Okhotsk," Tikhookean. Geol. **22** (4), 35–40 (2003) [in Russian].
19. "Cruise Report. Gregory. German–Russian Expedition for Geological/Geophysical Okhotsk Sea Research. RV *Akademik M. A. Lavrentyev* Cruise 27," Ed. by D. Nurnberg, B. V. Baranov, and B. Ya. Karp, GEOMAR Report **60**, 1997.
20. V. S. Vorob'ev, M. A. Voronkova, V. N. Pyatova, et al., "Atomic–Absorption Determinations of Silica, Iron, Calcium, Magnesium, and Manganese in Calc–Silicate Rocks and Bauxites," in *Methods of Chemical Analysis of Mineral Material* (VIMS, Moscow, 1977) [in Russian].
21. V. N. Pyatova, M. A. Voronkova, N. P. Ivanov, et al., "Atomic–Absorption Determination of Copper, Zinc, lead, Cadmium, Bismuth, Stibium, Cobalt, and Nickel in Rocks and Ores," in *Methods of Chemical Analysis of Mineral Material* (VIMS, Moscow, 1977), pp. 96–109 [in Russian].
22. M. Thompson and J. N. Walsh, *A Handbook of Inductively Coupled Plasma Spectroscopy* (Blackie, Glasgow, 1983; Nedra, Moscow, 1988).
23. G. M. Kolesov and V. V. Anikiev, "Specific Features of the Methodology of Sampling, Analysis, and Data Interpretation in Expeditionary Oceanology Investigations," Zh. Anal. Khim. **54** (9), 918–928 (1999) [J. Anal. Chem. No. 9, (1999)].
24. *Soils. Methods of Organic Matter Determination. GOST 26213-91. 1991* (Kom. Stand. Metrol. SSSR, Moscow) [in Russian].
25. A. I. Derkachev, A. I. Obzhirov, G. Borman, et al., "Authigenic Mineral Formation at the Occurrences of Cold Gas–Fluid Emanations at the Sea of Okhotsk Floor," in *Formation Conditions of Bottom and Sediments and Related Mineral Resources* (Dal'nauka, Vladivostok, 2002), pp. 47–60 [in Russian].
26. S. A. Gorbarenko, "Stratigraphy of the Upper Quaternary Sediments in the Central Part of the Sea of Okhotsk and Its Paleooceanology Based on Oxygen Isotopy and Other Methods," Okeanologiya **31** (6), 1036–1042 (1991).
27. L. N. Luchsheva, Extended Abstract of Candidate's Dissertation in (IBM DVO RAN, Vladivostok, 2004).
28. O. A. Mel'nikov and A. Ya. Il'ev, "New Volcanic Occurrences at Sakhalin," Tikhookean. Geol., No. 3, 42–48 (1989).
29. A. S. Astakhov, K. F. Sergeev, O. A. Mel'nikov, et al., "Dynamics of Defluidization of the Deep-Seated Cen-

tral Sakhalin Fault during Seismic Activation: Monitoring Results of the Southern Sakhalin Mud Volcano in July–August 2001," Dokl. Akad. Nauk **386**, 223–228 (2002) [Dokl. Earth. Sci. **386**, 742–748 (2002)].

30. *Geologiya SSSR. Tom XXXIII. Ostrov Sakhalin*, Ed. by A. V. Sidorenko (Nedra, Moscow, 1970), pp. 355–367 [in Russian].

31. *Tectonics and Hydrocarbon Potential of the Sea of Okhotsk*, Ed. by O. V. Veselov, A. Ya. Il'ev, V. E. Kononov, et al. (DVO RAN, Vladivostok, 2004), [in Russian].

32. O. A. Didenko, "Diagenetic Alterations of Gas-Hydrate-Bearing Sediments of the Sakhalin–Okhotsk Slope (Sea of Okhotsk)," in *Proceedings of 5th Interantional Scientific Symposium "Problems of Geology and Exploration of the Earth's Interior, Tomsk, Russia, 2001* (Tomsk Politekh. Univ., Tomsk, 2001), pp. 322–323 [in Russian].

33. A. S. Astakhov, K. Wallmann, and A. I. Botsul, "Geochemistry and Physicochemical Properties of Gas-Hydrate-bearing Sediments of the Sakhalin–Deryugin Slope, Sea of Okhotsk," in *Proceedings of International Conference "Conservation and Transformation of the Matter and Energy in the Earth's Crysophere, Pushchino, Russia, 2001"*, (Pushchino, 2001), pp. 43–44 [in Russian].

34. A. I. Obzhirov, V. A. Sosnin, and A. N. Salyuk, et al., *Monitoring of Methane in the Sea of Okhotsk* (Dal'nauka, Vladivostok, 2002) [in Russian].

35. S. C. Hsu, F. J. Lin, W. L. Jeng, et al., "Hydrothermal Signature in the Southern Okinawa Trough Detected by the Sequential Extraction of Settling Particles," Mar. Chem. **84**, 49–66 (2003).

36. S. A. Gorbarenko, V. Yu. Leskov, A. V. Artemova, et al., " Ice Cover of the Sea of Okhotsk during the Last Glaciation and Holocene," Dokl. Akad. Nauk **388**, 678–682 (2003) [Dokl. Earth. Sci. **389**, 208–211 (2003)].

37. D. W. Lea and E. A. Boyle, "Barium Content of Benthic Foraminifera Controlled by Bottom Water Composition," Nature **338**, 751–753 (1989).

38. T. M. Marchitto, W. B. Curry, and D. W. Oppo, "Zinc Concentration in Benthic Foraminifera Reflect Seawater Chemistry," Paleoceanography **15** (3), 299–306 (2000).

39. S. Honjo and S. J. Manganini, "Dichothermal Layer and Biological Export Production in the Sea of Okhotsk," in *Proceeding of the International Workshop on the Okhotsk Sea and Arctic; the Physics and Biogeochemistry Implied to the Global Cycles, Japan, 1996*, Ed. by M. Hisida (JAMSTEC–STA, 1996), pp. 103–110.

40. N. I. Seliverstov, G. M. Gavrilenko, and V. Yu. Kir'yanov, "On Signs of Recent Activity of Submarine Piip Voclano," Vulkanol. Seismol., No. 6, 3–18 (1989).